Challenges of Shape Memory Polymers: A Review of the Progress Toward Overcoming SMP's Limitations

Ingrid A. Rousseau
Materials and Processes Lab, General Motors Corp., R&D Center, Warren, Michigan 48090-9055

Many applications ranging from biomedical to aerospace have been proposed for the use of shape memory polymers (SMPs). To optimize SMPs properties for appropriately targeting such wide-spreading application requirements, it becomes necessary to understand the structure/property relationships in SMPs. The literature was reviewed and the recent advances made in the development of SMPs were determined to establish guidelines for composition and structure considerations for designing SMPs with targeted chemical, physical, and shape memory (SM) properties. It was concluded that covalently crosslinked glassy thermosets appear to be better SMP candidates because of their intrinsically higher modulus, greater thermal and chemical stability, higher shape fixity and recovery, and possibly their longer cycle life. However, material design allows for reaching comparable or better properties for all classes of SMPs. This emphasizes that optimization of SMPs requires application-specific molecular, structural, and geometrical design. Current techniques for improving stress recovery and cycle time, which compared to shape memory alloys are the two main limitations of SMPs, are extensively discussed. Understanding the relationships between the composition and structure of an SMP and its SM properties as well as its limitations enables one to better define the development areas for high performance SMPs. POLYM. ENG. SCI., 48:2075–2089, 2008.

INTRODUCTION

Smart materials encompass a wide variety of materials that are able to respond to specific stimuli [1]. Shape memory polymers (SMPs) are one class of smart materials that have attracted tremendous attention, especially in the last two decades. SMPs are polymers that can be deformed from a permanent shape to a temporary shape, that is, maintained until recovery to the starting permanent shape is commanded. These two shapes of the polymer result from the combination of an imposed deformation and the action of an external stimulus, most commonly a temperature variation above or below the SMP specific "transformation" or "switching" temperature. SMPs can be classified depending on their structures (thermosets vs. thermoplastics) and transformation temperatures (melting or glass transition temperatures) [2–4]. In the literature, SMPs based on common chemistries such as polyurethane (PU) [5–18], epoxy [19–25], polyolefin [26–28], as well as more exotic formulations such as partially dehydrochlorinated poly(vinyl chloride) [29], nylon/polyethylene graft copolymers [30], or poly (ether esters) [31–33] have been reported to show varying performances. This emphasizes the key role that polymer molecular design plays on tailoring the shape memory (SM) properties.

The increasing interest on SMPs over their more common shape memory alloy (SMA) counterparts relies mostly on their intrinsic advantages such as lower density, easier processing, lower cost, and larger attainable strains [5, 34, 35]. For certain polymers strains of up to 700% have been reported [5] compared to less than 10, 1, and 0.1% for SMA, SM ceramics, and glasses, respectively [36, 37]. However, some of the major drawbacks of SMPs are their relatively low modulus, which results in small recovery stresses/forces [5, 10, 12, 14, 18, 21, 22, 38, 39] (4–10 MPa against 200–400 MPa typically or higher for SMAs [10, 36]), their long response time [2, 11, 12, 40, 41] (much greater than the tens of milliseconds for SMAs of comparable size), and their seemingly low achievable number of cycles [12, 14, 42].

In this report, the recent advances made in the development of SMPs are reviewed in order to establish guidelines for composition and structure considerations necessary for designing SMPs with targeted performances. First, a brief definition of the SM effect is given. In addition, the techniques available for SM effect characterization are summarized. Because SM properties such as shape recovery have been quantified by various groups using slightly different expressions, they are discussed in light of the experimental procedure followed to collect them. Then, the impact of chemistry and structure on the SM behavior is discussed. In addition, advances reported for improving specific SM properties are described. Specifically, a focus is made on recovery stress and cycle

Correspondence to: Ingrid A. Rousseau; e-mail: ingrid.rousseau@gm.com
DOI 10.1002/pen.21213
Published online in Wiley InterScience (www.interscience.wiley.com).

time improvement. Finally, SMPs cycle life is briefly discussed in light of considerations from simplified constitutive models for predicting SM behavior.

SHAPE MEMORY EFFECT: DEFINITIONS AND CHARACTERIZATION

Shape Memory Polymers

SMPs are polymeric systems that can undergo temporary shape changes via mechanical deformation in their low modulus state and fix the temporary shape in their high modulus state, or revert back to their permanent, as processed shape upon application of an external stimulus. Ideally, if fixed, a temporary shape can be sustained indefinitely until the external stimulus is applied; although owing to the intrinsic viscoelastic behavior of polymers, this could only be theoretically achieved under extreme conditions, i.e., absolute zero temperature. Moreover, other factors, for instance material aging, should also be considered. Few researchers have studied shape fixity of the permanent shape over extended period of time, but Tobushi et al. [16] claimed dimensional stability of the temporary shape for their thermoplastic PU SMP foam at 30°C below its transformation temperature for up to 4 months.

Historically, temperature variation has been the external stimulus of choice because of the intrinsic thermal phase transitions occurring in polymers, i.e., the glass transition at which a material goes reversibly from a vitrified state to a rubbery state, or the melting transition at which a crystalline material looses its integrity and goes from a solid state to a liquid state. Concurrently, below and above the phase transition, a polymer goes from a high to low modulus state. Commonly, the transition temperature at which the shape change is observed in SMPs is referred to as "transformation" or "switching" temperature (T_{trans}). Although this review focuses on direct thermal activation, interesting developments that involved the use of alternate activation stimuli such as magnetic [43, 44] or electric fields [45], irradiation [34, 35, 46], and pH changes/ionization [2, 43, 47], amongst others, have been reported. In some instances, indirect heating is also achieved by inductive heating of SMPs using magnetic field [8], electric field, or irradiation [5].

SM effect has been attributed to the coexistence of a phase that allows for shape fixity through chemical or physical crosslinks and a phase that allows for reversibility through transitions such as a melting or a glass transition where the system goes from a low to a high molecular mobility [3, 20, 23]. Upon deforming in the rubbery state, the conformational rearrangement of the macromolecules along the deformation axis results in a network with reduced entropy. The latter is stored as energy upon cooling to the high modulus state where the deformed network configuration is frozen-in. Therefore, when an SMP in its temporary shape is heated under no stress/strain constraints to temperatures above its "reversible" phase transition, the increasing molecular mobility allows for the stored elastic energy to be released as a mechanical restoring force and for the material to recover its permanent original shape. If during heating the SMP is subjected to an external constraint, it exhibits a recovery stress, the extent of which is an important attribute for that SMP. Compared to those of SMAs, SMPs recovery stresses are low, typically 4–10 MPa against 200–400 MPa for SMAs [10], therefore driving some of the research toward their enhancement.

SMPs can be categorized into four classes depending on their chemical architecture and the origin of their transformation temperature [2, 4]. They can be (i) chemically crosslinked glassy thermosets, (ii) chemically crosslinked semicrystalline rubbers, (iii) physically crosslinked amorphous thermoplastics, and (iv) physically crosslinked semicrystalline block copolymers. This classification determines the mechanisms of shape fixity/recovery as well as of permanent shape setting of an SMP.

Although polymers are intrinsically viscoelastic materials, they do not all show SM properties. For this reason, SM should not be considered as an intrinsic polymer property [3, 11, 30]; however, some groups have stated the opposite [19, 27, 48]. In fact, adequate material and structural design is necessary for polymeric systems to exhibit SM behavior, that is, to restore the temporarily fixed residual inelastic deformation once reheated to the rubbery state. In contrast, ordinary polymers do not at all, or only to a low extent, recover from such residual inelastic deformation [26, 35]. For instance, Chun et al. [6] demonstrated that their (4,4′-methylene bis(phenyl isocyanate)/(poly(tetramethylene glycol) (MDI-PTMG)-based SMP showed increased shape retention and higher rate of recovery if a bimodal molecular weight distribution of soft segment along with a block-type arrangement of the copolymer was used in contrast to a random-type arrangement. Li et al. [17] investigated similar structure/property relationships for polycaprolactone/methane diisocyanate/butanediol (PCL/MDI/BDO)-based semicrystalline thermoplastic PU SMP. They concluded for their system that a lower limit of soft segment molecular weight in the order of 2000–3000 g/mol and a lower limit of hard segment content of 10% were necessary, only above which high strain recovery were attainable (i.e., 93–98%). Chemistry/structure/SM properties relationships have been experimentally investigated for other systems as well [11, 18, 30, 42]. Therefore, although SM effect could appear as an intrinsic polymer property, it results from the combination of material, structure, and morphology together with external conditions (strain, stress, temperature, and time). For every polymeric system, the careful determination of such a combination becomes crucial to produce high performance SMPs exhibiting extended cycle life, good chemical and thermal stability, excellent shape fixity/recovery, and adequate recovery speed.

 DOI 10.1002/pen

TABLE 1. Summary of the commonly imposed and measured parameters in a shape memory cycle characterization for both strain- and stress-controlled experiments.

	Strain-controlled		Stress-controlled	
SM cycle steps	Imposed parameters	Measured parameters	Imposed parameters	Measured parameters
Deformation	$\varepsilon_o \rightarrow \varepsilon_m^d$	$\sigma_o\ (\approx 0) \rightarrow \sigma_m^d$	$\sigma_o\ (\approx 0) \rightarrow \sigma_m^d$	$\varepsilon_o \rightarrow \varepsilon_m^d$
Cooling	$\varepsilon_m^d \rightarrow \varepsilon_m^s\ (=\varepsilon_m^d)$	$\sigma_m^d \rightarrow \sigma_m^s$	$\sigma_m^d \rightarrow \sigma_m^s\ (=\sigma_m^d)$	$\varepsilon_m^d \rightarrow \varepsilon_m^s$
Fixing	$\varepsilon_m^s \rightarrow \varepsilon_u = 0$	$\sigma_m^s \rightarrow \sigma_u$	$\sigma_m^s \rightarrow \sigma_u\ (\approx 0)$	$\sigma_m^s \rightarrow \varepsilon_u$
Free recovery	–	$\sigma_p \approx 0$	–	$\varepsilon_p \approx \varepsilon_o$
Constrained recovery	$\lvert\varepsilon_p\rvert > \varepsilon_o$	$\sigma_p > 0$	$\sigma_p > 0$	$\lvert\varepsilon_p\rvert > \varepsilon_o$

Shape Memory Properties: Definitions and Characterization

Shape Memory Cycle. The SM cycle of a thermally activated SMP represents its response when subjected to a thermomechanical cycle that allows for deforming and fixing of a temporary shape and recovering the permanent shape. SM cycles can be measured in tension using a tensile tester equipped with a thermally controlled chamber or a dynamic mechanical analyzer (DMA) as well as in compression using DMA. Bending deformations can also be performed and the deflection visually monitored. Although tension to high strains (≥100%) [6, 10, 14, 25, 26, 30, 38, 41] or bending at low strains are often analyzed [9, 21, 27, 39], less effort has been focused on SM behavior in compression [15, 16, 19, 20, 22]. Compression strains of 11–150% have been reported [15, 20]. To the author's knowledge shear or torsion deformation data of SMPs do not exist.

For simplicity, the steps involved in SM cycle characterization are described later in the case of a tensile deformation of a thermally activated SMPs, but a similar approach is applicable to other deformation types and activation stimuli. Depending on the instrument used for characterizing the SM behavior, the experiments can be performed in strain or stress-controlled modes. The SM cycles thereby measured will generate slightly different and complementary information; however, they all consist of four successive steps:

1. Deformation: The sample is deformed to a predetermined strain (ε_m^d) or stress (σ_m^d) at the deformation temperature (T_d) ≥ ($T_{trans} + \Delta T$). ΔT is often arbitrarily fixed at 20°C.
2. Cooling: Under the imposed deformation constraint, the sample is cooled from T_d to the setting temperature (T_s) ≤ ($T_{trans} - \Delta T$). Note that faster cooling generally prevents excessive stress or strain relaxation if any. The resulting strain or stress at T_s is denoted ε_m^s or σ_m^s, respectively. In a strain-controlled experiment $\varepsilon_m^s = \varepsilon_m^d$ and $\sigma_m^s \neq \sigma_m^d$, whereas in a stress-controlled experiment $\sigma_m^s = \sigma_m^d$ and $\varepsilon_m^s \neq \varepsilon_m^d$.
3. Fixing: The initial deformation constraint is released at T_s. If creep or spontaneous recovery has occurred upon unloading, the resulting unrecovered strain upon completion of the fixing stage is defined as ε_u ($\neq \varepsilon_m^s$) and the associated stress as σ_u.
4. Recovery: The temporarily deformed sample is heated back to above T_{trans}. If irrecoverable deformation was imparted to the sample during the cycle, then the resulting strain is defined as $\varepsilon_p \neq \varepsilon_o$. The corresponding stress (σ_p) is null for a nonconstrained recovery step and varies under constrained recovery.

In steps (i) through (iv) when operating under stress- or strain-controlled conditions, the stress (or force) is controlled and strain (or length) monitored or vice versa. For clarity purposes, the imposed and measured variables obtained in the case of both stress- and strain-controlled experiments are summarized in Table 1. In the case of bending deformation, strains are substituted by angle measurements. A graphical representation of the SM cycle is shown in Fig. 1. Note that the recovery step can be performed free of constraints or under load/strain to evaluate constrained strain/stress recovery.

Transformation/Switching Temperature, T_{trans}, and Response Temperature, T_r. The transformation/switching and the response temperatures both describe the temperature at which the SMP recovers its permanent shape. The former is defined as either the T_g or the melting transition temperature (T_m) responsible for the SM behavior of the SMP as dictated by its composition, such as $T_{trans} = T_m$ or $T_{trans} = T_g$. The T_s and the T_d required to fix the SMP temporary shape and to readily deform the SMP are generally imposed by using ($T_{trans} - \Delta T$) and ($T_{trans} + \Delta T$), respectively, with $\Delta T = 20$°C. However, semicrystalline SMPs achieve fixing of the temporary shape through crystallization at T_c with $T_c < (T_m = T_{trans})$. Therefore, the fixing of a temporary shape of a semicrystalline SMP requires cooling to even lower temperatures (e.g., T_{trans} −40°C instead of T_{trans} −20°C for glassy SMPs for which $T_{trans} = T_g$).

On the other hand, the response temperature (T_r) is measured either as the temperature at which 50% of the shape recovery has occurred [17, 30, 38] or as the maximum slope of the shape recovery versus temperature plot [26] such as $T_r = T_{[0.5R_f]}$ or $T_r = T_{\left[\frac{\partial R_r}{\partial t}=0\right]}$, respectively. A representation of the strain recovery and the shape

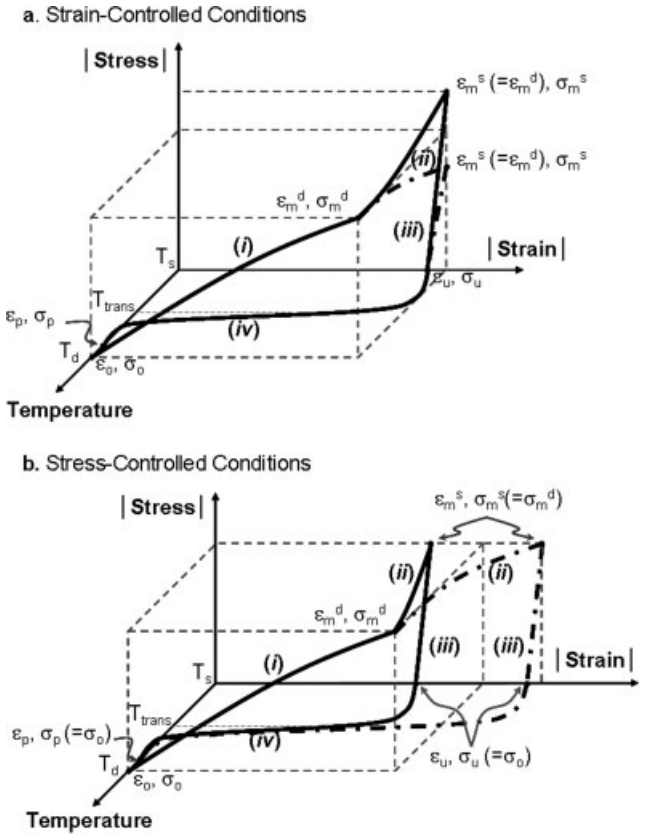

FIG. 1. Graphical representation of the typical shape memory cycle responses of an SMP undergoing a thermomechanical testing under (a) strain-controlled or (b) stress-controlled conditions. The various stages involved are: (i) deformation, (ii) cooling, (iii) fixing, and (iv) recovery. The dashed-dotted line and the solid line indicate the variation of the SMP response whether the effect of stress relaxation is dominant or not relative to the combined effect of the change in modulus above and below the SMP transformation temperature (T_{trans}) and the thermal contraction/expansion.

recovery as a function of temperature is shown in Fig. 2, where R_f represents the shape fixity of the SMP. Figure 2 depicts the case of T_r being calculated at 50% shape recovery. T_r may differ slightly from T_g or T_m and vary with experimental conditions such as time or heating rate [17, 26, 30, 38]. Similar considerations will have to be taken into account if determining the T_s of the temporary shape relative to T_r for a semicrystalline SMP network as those explained earlier for the determination of T_s relative to T_{trans}.

Shape Fixity, R_f [6, 9, 14, 16, 17, 25, 26, 30, 38, 39]. Shape fixity characterizes the ability of an SMP to fix the strain imparted in the sample during the deformation step after subsequent cooling and unloading. R_f is determined as the ratio of the strain resulting from the fixing step (ε_u) at the T_s (step (iii) in Fig. 1) to the strain of the sample upon completion of the deformation step (ε_m^d) at the T_d (step (i) in Fig. 1). It is expressed in the literature as:

$$R_f(\%) = \frac{\varepsilon_u(N)}{\varepsilon_m^d(N)} \times 100, \quad (1)$$

where N represents the cycle number.

In the case of strain-controlled experiments, a constant strain is maintained during the cooling stage (i.e., $\varepsilon_m^d = \varepsilon_m^s$); however, under stress-controlled conditions, the stress is kept constant and the strain varies (i.e., $\varepsilon_m^d \neq \varepsilon_m^s$) in response to changes in material properties (e.g., modulus, relaxation, thermal contraction/expansion). Therefore, care must be taken when evaluating R_f to use the appropriate strain value, ε_m^d. Because the changes in sample dimensions from T_d to T_s during the cooling stage as well as at T_s upon unloading are strictly related to material properties under the particular environmental conditions, they could potentially be relatively easily predicted.

Note that a few researchers have used somewhat different definitions for R_f [10, 20]; however, because the shape fixity quantifies the ability of an SMP to fix an imposed deformation at T_d, *Eq. 1* appears to best fit the definition.

Shape Recovery, R_r. Shape recovery characterizes the ability of an SMP to recover the accumulated strain during the deformation step after subsequent cooling and unloading upon reheating to the rubbery state. Several ways of expressing R_r have been reported. The first approach defines R_r as the ratio of the difference between the fixed strain after unloading the sample at T_s (ε_u) and that after completion of the recovery step (ε_p) to the fixed strain after unloading the sample at T_s (ε_u) [10, 14, 17, 25, 26, 30, 38]. A second approach defines R_r as the ratio

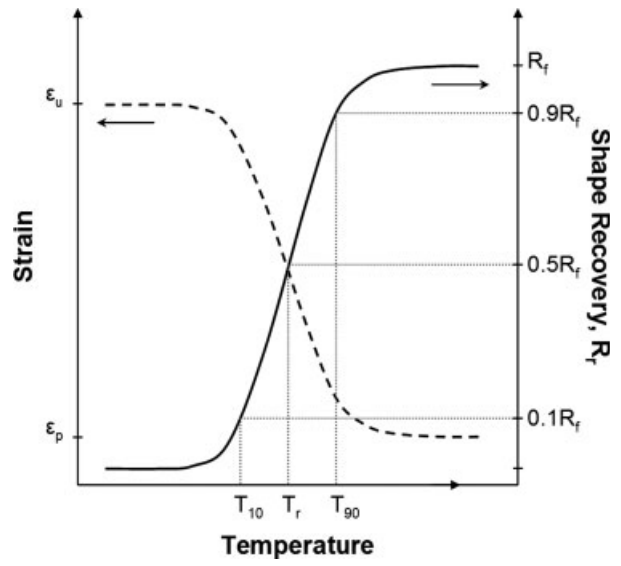

FIG. 2. Graphical representation of the recovery process of an SMP. The recovery rate and strain as a function of temperature are shown. The switching temperature, T_r is measured at 50% recovery. T_{10} and T_{90} correspond to the temperatures where 10 and 90% recovery is achieved, respectively. The strain evolution profile during recovery is also shown where the strain decreases from ε_p to ε_u (see Fig. 1).

 DOI 10.1002/pen

of the difference between the strain resulting from the deformation step (ε_m^d) and that after completion of the recovery step (ε_p) to the strain resulting from the deformation step (ε_m^d) [6, 9, 16, 39, 41]. Therefore, both approaches account for the spontaneous recovery, if any, that occurs upon sample unloading at T_s. At N number of cycles, the shape recovery can therefore be expressed by either one of the following expressions:

$$R_r(\%) = \frac{\varepsilon_u(N) - \varepsilon_p(N)}{\varepsilon_u(N) - \varepsilon_p(N-1)} \times 100, \quad (2)$$

or

$$R_r(\%) = \frac{\varepsilon_m^d(N) - \varepsilon_p(N)}{\varepsilon_m^d(N) - \varepsilon_p(N-1)} \times 100. \quad (3)$$

Another expression, equivalent to *Eq. 4* shown later, has also been used [48].

$$R_r(\%) = \frac{\varepsilon_u(N) - \varepsilon_p(N)}{\varepsilon_m^d(N) - \varepsilon_p(N-1)} \times 100 \quad (4)$$

In this case, it is interesting to note that the spontaneous recovery that may arise during the fixing stage at T_s upon unloading of the SMP is not accounted for in the recovery response. Indeed, this definition strictly compares the recovery occurring during the last heating stage of the SM cycle (recovery stage) to the deformation imparted to the sample after completion of the deformation stage at T_d.

In conclusion, it is necessary to consider the end-use application requirements when calculating the shape recovery because *Eqs. 2–4* will yield different values. Moreover, because *Eqs. 2* and *3*, in contrast to *Eq. 4*, both account for the spontaneous recovery at T_s as well as the heat-activated recovery, it is critical that researchers always report both values.

Recovery Speed, V_r [17, 26, 30, 38]. Recovery speed describes the percentage of recovery per unit time accomplished by an SMP in the temperature window where 10–90% recovery is accomplished between T_{10} and T_{90}, respectively (see Fig. 2). It is reported in percent strain per unit time and is expressed as follows:

$$V_r = \frac{0.8 R_f \varepsilon_u}{T_{90} - T_{10}} \times \left(\frac{dT}{dt}\right). \quad (5)$$

As can be seen from the abovementioned expression, V_r varies with heating rate; therefore, it is not an intrinsic property of the SMP but depends on both material properties and experimental conditions.

Shape Memory Cycle Life. The cycle life of an SMP is defined as the repeatability and durability of its SM properties over consecutive SM cycles. Therefore, the cycle life of an SMP defines the number of consecutive SM cycles it will be able to achieve without failure. Here, failure can either represent a noticeable decrease in the SM abilities in terms of shape recovery and shape fixity or an actual material failure. Although cycle life is a critical SM characteristic when considering the use of SMP applications requiring numerous cycles, the topic is rarely reported in the literature.

Shape Memory Cycle Time. SMP cycle time corresponds to the time required for an SMP to be transformed from its permanent shape to its temporary shape and reversibly to its permanent shape during a single thermomechanical cycle. Therefore, the cycle time represents the overall time necessary for the programing of an SMP temporary shape and the recovery of its permanent shape. As for cycle life, SM cycle time will be of importance when selecting SMPs for specific application requirements, whether short or long cycle times are required. The cycle time depends on material properties (i.e., viscoelasticity, thermal conductivity), geometric consideration and experimental conditions; therefore, it should always be reported in light of these other parameters to allow for appropriate selection.

Shape Memory Fill Factor, f_{sm}. The SM fill factor was recently defined by Liu et al. [48] as a quantity that would allow for a universal comparison of SM performance. In essence, the fill factor compares the actual/measured SM cycle of an SMP to that of the same SMP if it were to follow an ideal SM behavior (i.e., $R_f = R_r = 100\%$). It is determined graphically from the projection of the SM response in a strain versus temperature plot. It is calculated by first determining the area under the curves representative of the deformation and cooling stages between T_d and the temperature at which shape recovery starts. Then, the area under the curve representative of the recovery stage is calculated within the same temperature window and subtracted from the above value. This leads to what Liu et al. [48] refer to as $A_{\text{cross-hatch}}$. The same procedure is then performed for the same material if it was to follow an ideal behavior (i.e., no relaxation and/or instantaneous recovery) and leads to the quantity referred to as A_{ideal}. The fill factor is then calculated such as:

$$f_{sm} = \frac{A_{\text{cross-hatch}}}{A_{\text{ideal}}}. \quad (6)$$

Depending on the value of f_{sm}, SMPs can be categorized for this performance whether they exhibit (i) an ideal behavior with no relaxation at T_s and instantaneous recovery (i.e., $f_{sm} = 1$), (ii) excellent shape fixity and shape recovery with a finite recovery speed, (iii) excellent shape recovery and poor shape fixity, (iv) excellent shape fixity and poor shape recovery, and (v) poor shape fixity and shape recovery.

SMP Classification, Chemistry, and Performances

A large proportion of the heat-activated SMPs discussed in the literature are based on physically [6, 7] or covalently [8, 11, 12] crosslinked PUs. The coexistence of physically crosslinked hard segment regions or covalent crosslink points and of amorphous or crystalline soft segment regions imparts the SM behavior by acting as the fixed and reversible phase, respectively. Other common alternate chemistries include epoxy-based thermosets [19–22], crosslinked polyethylene [26], polynorbornene [27], and styrene–butadiene copolymers [49]. The four classes of SMPs are defined later. Typical examples of SMP compositions for each SMP class as well as a summary of their resulting SM properties as reported in the literature are included.

Class I: Chemically Crosslinked Glassy Thermosets. In such a system, the macromolecules are covalently linked and the resulting three-dimensional network exhibits a T_g below or above which the thermoset becomes reversibly glassy or rubbery, respectively. T_g governs the SM behavior in this case and the temporary shape is commonly formed at $T > T_g$ and fixed by cooling below T_g. The permanent shape is set by the covalent bonds of the three-dimensional network during processing.

For this class of materials, usually excellent shape fixity and recovery are observed due to the high modulus below T_g and excellent rubber elasticity above T_g. Indeed, the most common examples for this class of materials are epoxy-based SMPs that have been reported in the literature to show fixing and recovery of 95–100% when explicitly quantified [19–21]. Typically, such epoxy systems are commercially available thermoset epoxy systems with proprietary formulation. Some thermoset PU with trivalent or hybrid crosslinking have also been shown to exhibit recovery nearing 100% [11, 12]; however, no data on their shape fixity has been reported. All PU chemistries are based on relatively common formulations where diisocyanates hard segments are crosslinked with diols soft segments. A variety of crosslinkers may be used. The two formulations cited earlier use a11,1-trimethylol propane with an isocyanate group on each arm and an hybrid diol containing hydrolysable Si-OEt groups, respectively.

Very little data regarding cycle life is found in the literature; however, Xu et al. [12] reported that their Si—O—Si crosslinked hybrid PUs exhibited "no significant change of shape fixity and shape recovery rate due to repetition" over 50 thermomechanical cycles. Unfortunately, no quantitative data was shown to support that claim.

Class II: Chemically Crosslinked Semicrystalline Rubbers. Here, the permanent shape is again set by the chemical crosslinks formed during processing; however, a temporary shape is formed and fixed when the sample is deformed above the T_m of the crystalline regions and subsequently cooled below their crystallization temperature.

For this class of materials, there exists a wider range of shape fixity and recovery attainable that depends on the composition of the network compared to class I SMPs. Examples of such SMPs include crosslinked ethylene-vinyl acetate rubbers with 30–95% recovery depending on their composition [50]. Crosslinked polyethylene systems [26, 30] commonly used as heat shrink materials with fixing and recovery of up to 96 and 94%, respectively, and crosslinked polycyclooctene with almost complete (~100%) shape fixity and recovery have also been reported [27].

Therefore, class II SMPs can be tailored to optimize performance and reach shape fixity and recovery values of up to 95%. However, because the temporary shape is fixed through crystallization, the modulus in the "fixed" state is relatively low, in the order of 10^8 Pa, one order of magnitude lower than that for class I SMPs. Moreover, because intrinsically polymers show large thermal hysteresis between melting and crystallization transition temperatures, it is expected that class II SMPs would have to be cooled to lower temperatures relative to T_{trans} compared to class I SMPs to allow full crystallization for good shape fixity, potentially extending the SM cycle time.

Class III: Physically Crosslinked Amorphous Thermoplastics. For physically crosslinked amorphous thermoplastics, the SM behavior is attributed to the T_g of the soft segment regions and, therefore, a deformed shape obtained at $T > T_g$ is maintained by cooling below the glass transition. In contrast, the permanent shape of the network is provided by physical crosslinking of the hard segments through molecular interactions such as van der Waals, dipole–dipole interactions, or hydrogen bonding.

Physically crosslinked amorphous PUs represent the majority of this class of SMPs. Again, they are generally synthesized following common synthetic routes such as reacting diisocyanates and polyols with a diol or a triol as a crosslinker. Their shape fixity and recovery abilities have been reported to vary from 80 to 90% and 75 to 100%, respectively. Researchers have reported how the length and/or molecular weight distribution of soft segment and the hard segment content affect SM performance, especially with respect to recovery rate and to a lesser extent shape fixity and recovery speed. For example, as noted earlier, an MDI-PTMG-based PU showed increased shape retention and a higher rate of recovery if a bimodal molecular weight distribution of soft segment and a copolymer block-type arrangement were used [6]. Again, this emphasizes the need for optimizing material/structure/properties of SMPs in order to increase SM performance.

With regards to cycle life, Ohki et al. [14] reported on the SM behavior of a glass fiber reinforced PU, which underwent 60 consecutive mechanical cycles without failure and only a slight accumulation of residual strain as the cycle number increased; however, they tested only five consecutive thermomechanical cycles. In addition,

 DOI 10.1002/pen

Lin and Chen [42] tested their polyether-based PU SMP through 200 consecutive SM cycles. They observed an improvement in shape fixity and shape recovery for subsequent cycles with increasing cycle number although with a slight decrease in these properties relative to the initial, starting strain of the first cycle.

In conclusion, class III SMPs generally exhibit slightly lower SM performances compared to class I and II SMPs, specifically shape recovery and fixity. This is mainly explained by a loss in physical crosslinks integrity caused by mechanical deformation [6]. However, class III SMPs exhibit a relatively high modulus below T_{trans}, comparable to that of class I SMPs, in the order of 10^9 Pa.

Class IV: Physically Crosslinked Semicrystalline Block Copolymers. Very similar in their structure to class III SMPs described earlier, the physically crosslinked semicrystalline block copolymers exhibit SM behavior about the soft segment T_m, whereas retention of their permanent shape is achieved by physical crosslinking between hard segments through molecular interactions in crystalline regions.

Again, for this class of SMPs, the most commonly reported systems are PU-based with common chemistries involving for instance the use of polycaprolactone diol (PCL) as a soft segment, methylene diisocyanate (MDI) as a hard segment, and butandiol (BD) as the crosslinker [10, 17, 38]. Commercially available PU formulations have also been used [5]. For this class of SMPs, shape fixity and recovery have been stated to range anywhere from 65 to 96% and 56 to 100% depending on the composition (soft segments length and/or molecular weight distribution and hard segment content) [5, 10, 17, 38]. For instance, hard segment contents varying from 10 [17] to 33% [10] have been reported as optimum values for increased SM behavior in the PU systems described by Li et al. and Park et al., respectively. In addition, Li et al. also stated that their PCL/MDI/BD-based PU exhibited a lower limit of soft segment molecular weight, of 2000 to 3000 g/mol, for which SM performance were optimum [17].

Although SM behavior of class III and IV SMPs can be tailored to reach relatively high performance levels comparable to those of class I and II SMPs, they require SM training through a minimum of 2–3 cycles. Indeed, in contrast to covalently crosslinked SMPs, a significant irrecoverable strain generally results from the first completed SM cycle which persists through subsequent thermomechanical cycles. Therefore, an optimized behavior for a specific class IV SMP is achieved after the sample has been trained, that is, it has been cycled thermomechanically several times according to the application requirements prior to utilization.

Hydrogels. Although the above four classes of heat-activated SMPs represent the vast majority of SMPs described in the literature, other types of structures such as hydrogels have been shown to behave similarly. SM hydrogels are chemically crosslinked polymeric networks that are swollen in aqueous solutions. Although they appear similar to class I or II SMPs described earlier, the most common thermoresponsive hydrogels cited are *N*-isopropylacrylamide-based, which are activated around their lower critical solution temperature at which a volumetric transition of the network occurs through swelling or deswelling [51]. However, there are also class II hydrogels that have been reported such as acrylic acid/*n*-stearyl acrylate copolymer hydrogels that show SM behavior around 50°C, which corresponds to the T_m of the stearyl crystalline aggregates among the side chains that lock in the new temporary shape [52].

In addition, hydrogels can also be made pH, chemically, or electrically responsive, and also molecule specific (i.e., enzyme specific) [53]. Although interesting materials, their limitations are due to their need for a solvent that may constitute up to 90 vol% of the overall system and their low modulus in the order of hundreds of megapascal at most below their transformation temperature. As a result, these are usually intended for biomedical uses where they may offer better chemical and mechanical compatibility with their environment [2].

In conclusion, by comparing quantitative values reported in the literature for various SMPs, especially those of shape fixity and recovery, it appears that the SMPs of class I and II are the most reliable with: (i) reduced number of training cycles required to exhibit optimized SM behavior ($\leq$1 cycle), (ii) highest shape fixity and shape recovery (95+ %), and, also not mentioned earlier, (iii) intrinsically higher thermal stability and chemical resistance imparted by the covalent crosslinks.

Although there is no specific data discussed here on shape recovery speed, it has been reported that a narrower transition leads to a faster recovery [11, 12]. Melting transitions and their associated molecular relaxations often spread over narrower temperature windows than those associated with glass transitions; therefore, faster recovery rates may be achieved with crosslinked semicrystalline rubbers if designed appropriately [3]. However, the hysteresis between melting and crystallization transitions on heating and cooling could translate into longer overall SM cycle times requiring heating to higher temperatures or cooling to lower temperatures. Moreover, crosslinked semicrystalline rubbers generally exhibit lower elastic moduli than their glassy counterparts below their transition of interest for use as an SMP; therefore, this is also an important factor to consider for the desired end-use applications. This emphasizes the importance of defining the requirements for each application in order to select the appropriate SMP chemistry and design the appropriate SMP systems.

Cycle life of SMPs is rarely discussed in the literature. Indeed, whether targeted for medical or aerospace applications, it appears that SMPs are often intended for a single-cycle application. Only a few articles reported on

repeatability above the commonly used 3–5 consecutive cycles of class I and III SMPs [12, 14, 16, 42].

Finally, although SMPs show tremendous advantages compared to other SM materials such as alloys or ceramics, especially in terms of their ease of use and processing, low cost, and large attainable strains (2+ order of magnitude higher), their recovery stresses are comparatively small (4–10 MPa) when considering their use in constrained environments.

The following section focuses on discussing the advances made toward the resolution of the abovementioned weaknesses of SMPs, specifically cycle time, cycle life, and recovery stresses.

SMP Limitations and Improvement

We mentioned earlier that the main disadvantages of SMPs over their alloy, ceramic, or glass counterparts reside mainly in their lower recovery stress ($\leq$10 MPa), their lower recovery speed/response time (up to tens of seconds in open air depending on their size vs. tens of milliseconds for SMAs), and their possibly lower achievable cycle life (200 cycles vs. 100–10^6 reported for NiTi SMA depending on deformation conditions), although the latter has only rarely been investigated in the literature.

In this section, an attempt is made to provide guidelines based on the results described in the literature to circumvent these limitations.

Recovery Stress

The low recovery stresses exhibited by polymeric systems over their alloy, ceramic, and glass counterparts are mainly due to their intrinsically lower modulus, in the order of 10^8–10^9 Pa below the switching temperature and 10^6 Pa above it. Therefore, increasing recovery stresses has been sought by increasing SMPs stiffness or elastic modulus. This has been achieved by increasing crosslinking density, reinforcing polymer systems by inclusion of fillers, or by providing mesomorphic characteristics to SMPs. Indeed, Jeong et al. [18] introduced mesogenic units in their thermoplastic PU so as to form a liquid crystalline phase in the rubbery region above the soft segment melting point resulting in an increase of the rubbery modulus from 34 to 283 MPa while maintaining acceptable shape fixity and recovery (≥90%) after training. There was no mention however of the gain in recovery stress achieved.

Also, modest increases in rubber modulus, following the theory of rubber elasticity, have been achieved by increasing crosslink density such as:

$E'_R = 3\nu_e RT$, where E'_R is the storage modulus in the rubber plateau region, ν_e the crosslink density, R the gas constant, and T the temperature. Indeed, Xu et al. [12] investigated the behavior of their thermoset hybrid PU where the crosslinks are based on Si—O—Si bonds (Note that these may also act as reinforcing inorganic fillers). They chose their systems in order to obtain SMPs with high storage modulus ratio below and above T_{trans} ($E'_{T<T_{trans}}/E'_{T>T_{trans}}$) and high storage modulus above T_{trans} ($E'_{T>T_{trans}}$). Indeed, they indicated that pristine SMPs with $E'_{T<T_{trans}}/E'_{T>T_{trans}} > 100$ are preferred because they favor deformation at high temperature and fixing at low temperature. Moreover, they also indicated that $E'_{T>T_{trans}} \geq 10^6$ Pa are advantageous for shape recovery through higher stress reservation of deformation during cooling/fixing. As expected, $E'_{T>T_{trans}}$ of their SMPs increased with increasing crosslink density from 3.85 to 16.34 MPa, while the amplitude of tan δ decreased. They concluded that both the higher modulus at $T > T_{trans}$ and the lower tan δ at higher crosslink density were accountable for the lower shape fixity and faster recovery. Unfortunately, in their study, the effect of crosslinking is coupled with other factors, for instance, the improvement of network homogeneity which would also result in faster recovery through narrower relaxation time distribution at $T_{trans} = T_g$. In all cases, recovery strains attained 100% independently of crosslink density.

The most common way of increasing elastic modulus, however, is to include fillers in the polymer matrix. Carbon particles [38], carbon fibers or fabrics [39], silicon carbide particles [21, 22], glass fibers [14], nanoclays [10], and, more recently, carbon nanotubes [5] (CNTs) are amongst examples of such fillers. For ease of comparison, the reported effects of some such fillers on SM properties are summarized in Table 2. Although the addition of fillers increases the rubbery modulus, the effect on the modulus below the switching temperature ($T_{trans} = T_g$ or T_m) is much less, therefore, resulting in a reduced $E'_{T<T_{trans}}/E'_{T>T_{trans}}$. Indeed, as stated in the reviewed publications, a decrease of the latter ratio leads to a decrease in shape recovery and/or shape fixity while increasing stress recovery. However, one can see that after sufficient training cycles (~3 cycles), shape fixity and shape recovery can be increased to above 80% relative to the preceding cycle. On one hand, the amplitude of stress recovery is directly related to the variation in modulus above T_{trans} resulting from the addition of fillers; on the other hand, the often observed decrease in shape recovery and/or increase in shape fixity is related to the presence of embedded fillers that may arrange into networks counteracting and/or reinforcing the SM behavior of the polymer network.

Finally, without addition of fillers or changes in polymer structure and/or chemistry, increase in stress recovery has been reported for SMPs at T_d below T_{trans} where $T_{trans} = T_g$. Indeed, Liu et al. [21] reported an increase in stress recovery from about 1 to 2 MPa by deforming their epoxy SMP at $T_d \approx T_{trans} - 30$°C. This is due to the fact that to reach identical strain levels at T_1 and T_2 such as $T_1 < T_{trans} < T_2$ the stress levels required are such as $\sigma_1 > \sigma_2$. This results in an increase of the stored energy and an overshoot of the stress recovery response around the switching temperature of the SMP. However, the final

 DOI 10.1002/pen

TABLE 2. Summary of the effect of inorganic filler inclusion on shape memory polymers with respect to resulting shape fixity, shape recovery, and recovery stresses.

Filler type	SMP type	Filler loading	Shape fixity	Shape recovery	Modulus	Recovery stress	Ref
Carbon nanotube (CNT)[a]	PU (morthane®)	1–5 vol%	Increases from 56 to 70% (5% CNT)—enhance strain induced crystallization	~100% after 3rd cycle	$2E'^{p}_{R} < E'^{f}_{R} < 5E'^{p}_{R}$	Up to 50% increase (0.6–1.4 MPa)	[5]
Nickel zinc ferrite particles[b]	Ester-based thermoset PU	1–20 vol%	No significant change	No significant change	10 vol% loading: 56% increase at $T < T_g$ 24% increase at $T > T_g$	N.A.	[8]
Nanoclay	Thermoplastic PU	1–5 wt%	Reduced from 96 to 93% with 5 wt% clay	Pristine: ~100%, 1–3 wt% clay: ~90%, 5 wt% clay: ~85%	5.2–12.2 MPa with 5 wt% clay	+ 20% (~3.8–4.8 MPa with 1 wt% clay)	[10]
Glass fiber	Thermoplastic PU	10–30 wt%	N.A.	1st cycle: ≤65% (T-dependent) 3rd + cycles: ~80–90%	$T < T_g$: from ~1 to 2 GPa $T > T_g$: from ~1 to 20 MPa	N.A.	[14]
SiC	Thermoset epoxy	20 wt%	~100%	100% if no constraints	$E'^{f}_{R} \sim 2E'^{p}_{R}$	~2x with filler but still <2 MPa (strains <20%)	[21]
SiC	Thermoset epoxy	20 wt%	~70% 1st cycle	N.A.	N.A.	31 vs. 5–6 MPa for pristine SMP	[22]
Mesogenic hard segments[c]	Thermoplastic PU	20–50%	~90%	1st cycle: ~80%, 2nd+ cycle: >95%	From 34 to 283 MPa	N.A.	[18]

E'^{f}_{R}: Storage modulus at rubbery plateau for the filled SMP; E'^{p}_{R}: storage modulus at rubbery plateau for the pristine SMP.
N.A., not data available.
[a] Thermal actuation through IR irradiation.
[b] Thermal actuation through inductive heating by thermoregulation using Curie temperature of particles.
[c] Note: This is part of the copolymer and is not a filler.

recovery stress scales linearly with the stress/strain response at high temperatures as it does when deformed at $T_d > T_{trans}$. However, deforming a sample at $T < T_{trans}$ generally leads to a larger spontaneous strain recovery than deforming it at $T > T_{trans}$ and subsequently cooling it below T_{trans} before unloading [19].

Several ways of increasing elastic modulus in order to reach higher recovery stresses have been discussed. Although increasing crosslink density and adding inorganic fillers to the polymer matrix yield moderate to large recovery stress improvements, less orthodox methods such as changing the polymer chemistry to impart mesomorphism or simply changing the deformation conditions (thermal or mechanical) have shown comparable effects. Whether changing the structure, chemistry, or the deformation conditions of an SMP, optimization of the system is required to maintain the overall good SM properties.

Cycle Time

As the cycle time of an SMP encompasses the time required for the thermomechanical programing of its temporary shape and the time necessary for the recovery of its permanent shape, it varies with: (i) the width of the thermal transition responsible for the SMP transformation and the hysteresis of the transformation temperature responsible for the observed SM behavior and (ii) the heat transfer of the SMP. The latter depends on thermal conductivity, heat capacity, mass, and volume of the SMP. Therefore, geometric design optimization is necessary to achieve minimal size and shape requirements for desired/targeted end-properties.

Width of the SMP Thermal Transition. The width of the thermal transition is governed by the distribution of relaxation times associated with molecular mobility at the switching temperature, which in turn depends on chain length, molecular interactions, and constraints. Whether the transformation temperature is a glass or a melting transition, the microstructure will require appropriate design to allow for sharp transitions. Buckley et al. [11] calculated normalized retardation spectra from creep master curves and correlated the latter to the shape recovery process of their system (thermoset PU). In general, they found that the recovery speed scaled with the width of the distribution and that the width of the thermal transition decreases with decreasing soft segment chains, which leads to a more "homogeneous" network with narrower retardation time distributions. This is in good agreement with results from other groups [12, 40].

Also, although SMPs can be actuated about T_g and T_m, melting transitions are usually narrower than glass transitions [3]; therefore, class II and IV SMPs could be expected to have faster fixing and recovery. However, because melting and crystallization also exhibit a large thermal hysteresis on heating and cooling, which increases further with increasing cooling/heating rates, the overall thermomechanical cycle associated with the deformation, fixing, and subsequent recovery of these SMPs may still be longer than that of class I and III SMPs even at fast cooling/heating rates. Moreover, very fast cooling rates could jeopardize the extent of crystallization of the T_m-activated SMPs necessary for them to exhibit their expected shape fixing.

Heat Transfer Consideration. Because changing the temperature is a means of reversibly going from the permanent to temporary shape for heat-activated SMPs, heat transfer, and therefore thermal conductivity are of prime importance when considering SM cycle time. Indeed, Liu and Mather [40] indicated the existence of two zones during shape recovery: (i) a thermal diffusion zone dictated by heat transfer through sample geometry and thermal conductivity, followed by (ii) a shape recovery zone controlled by the viscoelastic properties of the material.

The thermal conductivity of polymers is very low [$\leq$0.3 W/(K m)] relative to that of typical SMA. For instance, Nitinol® exhibits a thermal conductivity of about 18 W/(K m), over 60 times greater than that of SMPs. Low thermal conductivity is a limitation for SMPs and, although many efforts have focused on increasing the thermal conductivity of polymers, work for improving SMPs thermal conductivity has only recently been initiated. Although for thermal conductivity enhancement the same principles will hold true for a generic polymer and an SMP, it is important to study the effect of the changes imparted to the matrix on the SM properties so that thermal conductivity and SM behavior are simultaneously optimized. Increasing the thermal conductivity of polymers and/or SMPs has been commonly achieved with addition of inorganic fillers of intrinsically higher thermal conductivity, such as carbon-type fillers, CNTs [54], glass fibers, metal particles [55], silicon carbide, boron nitride [40], amongst others [41.56]. Note that, although it has been shown that the thermal conductivity of a polymer is greatly enhanced by adding fillers with up to 100 times greater thermal conductivity, it has been predicted that fillers with thermal conductivities greater than 100 times that of the polymer matrix would not significantly further increase the thermal conductivity of the resulting composites [56]. Unfortunately, although the thermal conductivities, and potentially, the cycle time of the resulting composite SMPs can be optimized by this method, the elastic modulus of SMPs increases due to the reinforcing effect of the fillers, resulting in sometimes dramatically reduced shape recovery abilities. This is a similar consequence to what was also observed when adding fillers for stiffness enhancement of the SMP. For instance, Razzaq and Frormann [41] noted that the shape recovery of their SMP is reduced from 96 to 70% by addition of a highly thermally conductive aluminum nitride filler (40 wt%), while the conductivity at room temperature was increased from 0.12 to 0.44 W/(K m). Other reports focus solely on the enhancement of thermal conductivity of polymers

 DOI 10.1002/pen

upon addition of specific fillers. Some of the most concluding results are indicated thereafter. Weidenfeller et al. [55] investigated the effect of talc, cupper, magnetite, and ferrite on thermal conductivity and thermal diffusivity of PP-based composite. The largest increase in thermal conductivity, from 0.27 to 2.50 W/(K m), was observed after the addition of 30 vol% of talc as rationalized through better interconnectivity of the fillers. In addition, because of their low density, these composites also showed a propensity for faster cooling. Chen and Ting [57] reported an extraordinary increase in thermal conductivity, from 0.1 to 695 W/(K m), for their epoxy polymer composite by incorporating 56 vol% of heat-treated vapor grown carbon fibers. They largely attributed this to the orientation and extremely high aspect ratio of the fibers. Even at relatively low loading of 14 vol%, k increases in both parallel and perpendicular directions to the vapor grown carbon fibers from 0.1 to 198 and 3.9 W/(K m), respectively, while maintaining a low composite density of 1.27 g/cm^3.

Other exceptionally large increases in thermal conductivity of composites have been expected upon incorporation of CNTs into polymer matrices. Indeed, (CNT) fillers have also been increasingly studied because of their low loading requirement compared to conventional fillers (<2 wt% vs. ≥20 wt%) and their potential for imparting not only increased thermal conductivity to the polymer host but also enhanced mechanical properties and electrical conductivity. However, the influence of CNT loading on the thermal conductivity of CNT-based composites is quite different from what is observed with conventional fillers. In contrast to conventional composites, the thermal conductivity of CNT composites does not exhibit the typical percolation behavior and increases more or less linearly with CNT volume fraction. However, percolation thresholds ranging from 0.002 to 11 wt% have been reported via electrical conductivity measurements [58, 59]. This implies that at slightly higher concentrations, the viscosity of the CNT-based composites would become unmanageable during processing, and most likely lead to poor dispersion, agglomeration, and/or premature degradation. This is unlike that of conventional composites that can easily incorporate 30–40 wt% of fillers. Gojny et al. [54] discussed the influence of specific surface area, aspect ratio, functionalization, and interfacial interactions on thermal conductivity of an epoxy-based composite incorporating single-, double-, and multi-wall CNT (SWCNT, DWCNT, MWCNT, respectively). They found that the increase in thermal conductivity increases with decreasing specific surface area. As such, the effect increases in accordance with the following sequence: MWCNT > DWCNT > SWCNT. However, the effect was limited with only a slight increase in thermal conductivity from 0.242 to 0.251 for 0.3 wt% of MWCNT. They also concluded that for nanofillers, the effect of aspect ratio is minimal in comparison to the effect of the surface area that promotes interfacial boundary phonon scattering. It becomes of importance for larger scale fillers when interfacial area is reduced. Finally, they indicated that poor interaction between CNT and polymer matrix appeared to enhance the thermal conduction. This contradicts general requirements for improving mechanical properties with CNTs [58–60]; therefore, CNT fillers may not be appropriate for incorporation in SMPs. These results are in accordance with many other publications on the subject. Indeed, thermal conductivity in CNT-based composites is believed to be dominated by phonon excitation [58, 61–64]. Because the ratios of thermal conductivities of CNT to polymer matrix are quite low, in the order of 10^4, the heat transfer involves both the matrix and the CNTs, as opposed to electronic transfer which preferentially occurs through CNTs [65–67]. Because of the generally limited interaction between CNT and polymer, the energy contained in high frequency phonon modes in the CNTs is required to be transferred to low frequency phonon modes through phonon–phonon coupling in order to travel through the polymer matrix which results in exceedingly low interfacial thermal conductance. This explains why in CNT buckypaper, where air is the matrix, the effective thermal conductivity is only in the order of 10–30 W/(K m) as opposed to 3000 or 6600 W/(K m) predicted at room temperature for individual MWCNT or SWCNT, respectively [58, 59, 62, 64, 68, 69]. To decrease interfacial thermal resistance, functionalization of CNT has been attempted; however, it is found that there exists a competing effect between functionalization and defect creation. Indeed, although CNT functionalization reduces the thermal interfacial resistance between polymer matrix and CNT, it also creates defects on the CNT walls that act as new phonon scattering sites [64, 70]. In turns, there appear to be optimum functionalization and aspect ratio values at which the composite thermal conductivity enhancement will be the best. This supports the experimental results obtained by Gojny et al. mentioned earlier. Outside of these values, the composite thermal conductivity can remain unchanged, only slightly increased, or even reduced compared to that of the pristine polymer matrix. Among CNT fillers, MWCNTs have been reported to be better candidates for increasing thermal conductivity of CNT-based composites [54, 71]. In contrast to the largely adopted belief that interfacial resistance plays an important role in the smaller than expected values of thermal conductivity of CNT-based composites, Bagchi and Nomura [71] reported that in MWCNT composites the lower than expected composite thermal conductivity arose mainly from the fact that the phonon conduction occurs mostly through the outer layer of the CNT, not involving the inner layers. Again, they observed an effect of tube diameter on overall conductivity such as smaller diameter tubes (i.e., higher aspect ratio) yielded increased thermal conductivity. In addition, Chen et al. [72] through simulation work indicated that it is the interfacial resistance that impedes thermal conductivity enhancement the most, rather tube-end heat transfer.

In conclusion, the SM cycle time can be decreased by optimizing the polymer chemical and structural arrangement in order to synthesize a "homogeneous" network exhibiting a narrower transition temperature window. Although narrower transition temperature windows lead to faster recovery, it has been reported that the latter depends mostly on the heat transfer, and hence, sample geometry and thermal conductivity, rather than on the material viscoelastic properties. Moreover, polymers intrinsically act as insulators and it is necessary to increase their thermal conductivity in order to improve their SM cycle time. Many studies aiming at applications in microelectronics have attempted this. The general approach consists of loading the polymer system with highly conductive fillers; however, other requirements are necessary to witness appropriate k increase such as fillers intrinsic conductivity, filler content, size, aspect ratio, density, surface area, and filler/polymer matrix interaction (i.e., wetting). Unfortunately, filler loading for improved thermal conductivity may lead to decreased mechanical properties.

As mentioned earlier, the thermal conductivity can be significantly increased by adding inorganic fillers with thermal conductivity up to 100 times greater than that of polymer matrix. The greatest improvement in thermal conductivity occurs for filler content at or above the percolation threshold (higher for spherical than elongated particles). Although intrinsically CNTs exhibit better physical properties than conventional fillers, comparing results between composites incorporating conventional fillers or CNTs indicates that the former would be preferable for use in SMPs unless new compatibilization techniques are discovered for incorporating CNT in a polymeric matrix.

Cycle Life

The cycle life of an SMP corresponds to the repeatability and durability of its properties over consecutive SM cycles. To the author's knowledge, extended cycle life has not been discussed in the literature. Most likely, this is attributed to the fact that most applications for which SMPs are intended, thus far, require only a single cycle to be performed, such as biomedical applications. For instance, SMPs used as surgical implants for thrombus removal after ischemic stroke would only require single deployment of their cork screw permanent shape after the straight (rod temporary) shape was inserted through the vascular occlusion [7]. After a single use (i.e., thrombus removal) such an SMP is discarded.

Cycle life is generally tested over 3–5 SM cycles. Three reports were found that tested for greater cycle numbers: 50 thermomechanical cycles [12], up to 60 mechanical cycles (no change in temperature) [14], and 200 SM cycles [42]. They all observed no significant change in properties with increasing cycle number [12, 14] or even a slight increase in shape recovery from cycle-to-cycle for increasing cycle number (99+ %) [42]. These numbers are far from the repeatability reported for SMAs, which depending on the conditions, can achieve up to 10^6 cycles without SM properties reduction. In each case, the higher cycle numbers reported were achieved at low strains using a bending tests to quantify SM behavior [12, 42] or static tensile tests at strains below 4% [14]. Although no data was found for higher life cycle, it does not mean that they cannot be achieved, only that they were not investigated.

In parallel to experimental studies, constitutive models for describing/predicting SM behavior have been proposed [13, 20, 73, 74]. They are all based on low strains deformations that fall within the linear viscoelastic region of the polymer at its T_d. These correspond to strains lower than 20% that are considerably smaller than those often used in experimental studies of SMPs of 100+ %. The various models thereby developed are in fairly good agreement with experimental data for the same strain levels. This seems to indicate that under these conditions, an SMP could potentially go through numerous cycles without losing its SM characteristics, although none of the models reviewed take into account the aging process of the SMP undergoing successive thermomechanical cycling. Theoretically, in the linear viscoelastic region, no irreversible transformation should occur under the applied stress, whereas above the linear region irreversible conformational changes such as disentanglement occur that could result in irreversible deformations at the macroscopic scale.

In conclusion, both experimental and theoretical approaches in studying SM behavior suggest that deformation conditions (i.e., time, strain/stress, strain/stress rates, temperature) affect cycle life of SMP properties, and hence their effect on the SM response should be further investigated and understood in order to appropriately design application-specific, high-performing SMPs.

CONCLUSIONS

Although viscoelasticity is intrinsic to polymers and is the basis of SM effect in polymers, "true" SM effect requires appropriate material and structural design and, therefore, is not intrinsic to polymers.

The various quantities that characterize the SM behavior namely, the shape fixity (R_f), shape recovery (R_r), switching and response temperature (T_{trans} and T_r, respectively), recovery speed (V_r), and fill factor (f_{sm}) were reviewed and their physical significance briefly discussed. Because the values of shape recovery and shape fixity are closely related, they should be determined simultaneously and the definitions used to calculate their values clearly stated.

The various SMP classes were also reviewed. They are defined as (class I) chemically crosslinked glassy thermosets, (class II) chemically crosslinked semicrystalline rubbers, (class III) physically crosslinked amorphous thermoplastics, and (class IV) physically crosslinked

 DOI 10.1002/pen

semicrystalline block copolymers. After inspection of the SM properties exhibited by various representative of each class of SMPs, it appears that class I and II SMPs are better candidates for SMP applications. Their benefits reside in their minimum SM training requirement (≤ 1), their excellent shape fixity and recovery, nearing 100%, their intrinsically better chemical and thermal stability, and their potentially, better cycle life (i.e., repeatability/durability). Moreover, class I SMPs offer intrinsically shorter overall cycle times over class II SMPs ($T_{trans} = T_g$ instead of T_m) as well as higher moduli below T_{trans} ($\sim 10^9$ vs. $\sim 10^8$). A brief review of hydrogel-based SMP was also presented.

Solely in terms of SM properties, the disadvantages of SMPs compared to SMAs reside in their lower recovery stress, longer cycle time, and their lower cycle life. The literature was reviewed to investigate alternative routes to overcome these limitations. Because the recovery stress is governed by the elastic modulus of the material and the external mechanical constraint, routes followed to increase recovery stresses include the addition of fillers, the increase in crosslink density, or the creation of polymorphism. Additionally, deforming at $T < T_{trans}$ has also been proven effective at increasing recovery stress. The recovery speed and overall SM cycle time are governed by the width of the thermal transition at T_{trans}, the hysteresis on heating and cooling of the thermal transition responsible for the SM effect activation, and the SMPs thermal conductivity. The former decreases with network perfection/homogenization, whereas the latter is commonly increased by the addition of fillers. The hysteresis on cooling and heating of the SMPs thermal transition is mostly observed for melting/crystallization transitions, which indicates that T_m-activated SMPs may intrinsically exhibit longer cycle times. However, although the addition of fillers has generally proven beneficial for increasing recovery stress or thermal conductivity, its impact on SM properties can be detrimental. In fact, although it has been shown that adding fillers to an SMP usually improves shape fixity, it also reduces shape recovery, sometimes dramatically.

Finally, the cycle life was found to be rarely tested. Results from experimental data and from simplified constitutive models at low strains (<20%) appear to indicate that cycle life could be significantly increased by keeping the deformation in the domain of strains confined to the linear viscoelastic region of the polymer, where stress and strain are directly proportional and where no irreversible conformational changes of the polymer network take place. Again, although the addition of fillers may considerably improve the cycle time and recovery stress, it may also negatively impact cycle life.

ACKNOWLEDGMENTS

The author thank Hamid Kia, Nilesh Mankame, Tao Xie, and Will Rodgers from the GM Corporation for their helpful discussions regarding shape memory materials, particularly shape memory polymers.

NOMENCLATURE

α	Thermal diffusivity
CNT	Carbon nanotube
C_p	Heat capacity
DMA	Dynamic mechanical analyzer
DWCNT	Double wall carbon nanotube
E_R'	Storage modulus in the rubber plateau region
$E'_{T<T_{trans}}$	Storage modulus at a temperature below the transformation temperature
$E'_{T<T_{trans}}$	Storage modulus at a temperature above the transformation temperature
f_{sm}	Shape memory fill factor
K	Thermal conductivity
MWCNT	Multiwall carbon nanotube
v_e	Crosslink density
PU	Polyurethane
ρ	Density
R	Universal gas constant
R_f	Shape fixity
R_r	Shape recovery
SM	Shape memory
SMA	Shape memory alloy
SMP	Shape memory polymer
SWCNT	Single wall carbon nanotube
t	Time
T	Temperature
T_{10}	Temperature at 10% shape recovery
T_{90}	Temperature at 90% shape recovery
T_c	Crystallization transition temperature
T_d	Deformation temperature of a shape memory polymer
T_g	Glass transition temperature
T_m	Melting transition temperature
T_r	Response temperature of a shape memory polymer
T_s	Setting (fixing) temperature of a shape memory polymer
T_{trans}	Transformation/switching temperature of a shape memory polymer
V_r	Recovery speed of a shape memory polymer
ε	Strain
ε_o	Initial strain applied or measured on polymer in a shape memory cycle
ε_m^d	Maximum strain reached by a shape memory polymer as a result of the deformation step at T_d during the shape memory cycle
ε_m^s	Strain reached by a shape memory polymer after deforming at T_d and subsequently cooling to T_s under load during the shape memory cycle
ε_p	Unrecovered strain due to permanent plastic deformation of the shape memory polymer at the end of the shape memory cycle after recovery

ε_u Strain of a shape memory polymer after the unloading step at the setting temperature

σ Stress

σ_o Initial stress applied or measured on polymer in a shape memory cycle

σ_m^d Maximum stress reached by a shape memory polymer as a result of the deformation step at T_d during the shape memory cycle

σ_m^s Stress reached by a shape memory polymer after deforming at T_d and subsequently cooling to T_s under load during the shape memory cycle

σ_p Unrecovered stress due to permanent plastic deformation of the shape memory polymer at the end of the shape memory cycle after recovery

σ_u Stress of a shape memory polymer after the unloading step at the setting temperature

REFERENCES

1. P.T. Mather, *Nat. Mater.*, **6**, 93 (2007).
2. I.A. Rousseau, Development of Soft Polymeric Networks Showing Actuation Behavior: From Hydrogels to Liquid Crystalline Elastomers, Thesis, University of Connecticut, 2004.
3. M. Behl and A. Lendlein, *Mater. Today*, **10**, 20 (2007).
4. C. Liu, I.A. Rousseau, H. Qin, and P.T. Mather, *Proc. First World Cong. Biomim.*, (2002).
5. H. Koerne, G. Price, N. Pearce, M. Alexander, and R.A. Vaia, *Nat. Mater.*, **3**, 115 (2004).
6. B.C. Chun, T.K. Cho, and Y.-C. Chung, *J. Appl. Polym. Sci.*, **103**, 1435 (2007).
7. W. Small IV, M.F. Metzger, T.S. Wilson, and D.J. Maitland, *IEEE J. Select. Top. Quant. Electron.*, **11**, 892 (2005).
8. P.R. Buckley, G.H. McKinley, T.S. Wilson, W. Small IV, W.J. Benett, J.P. Bearinger, M.W. McElfresh, and D.J. Maitland, *IEEE Trans. Biomed. Eng.*, **53**, 2075 (2006).
9. J.R. Lin and L.W. Chen, *J. Appl. Polym. Sci.*, **73**, 1305 (1999).
10. F. Cao and S. Jana, *Polymer*, **48**, 3790 (2007).
11. C.P. Buckley, C. Prisacariu, and A. Caraculacu, *Polymer*, **48**, 1388 (2007).
12. J. Xu, W. Shi, and W. Pang, *Polymer*, **47**, 457 (2006).
13. H. Tobushi, K. Okumura, S. Hayashi, and N. Ito, *Mech. Mater.*, **33**, 545 (2001).
14. T. Ohki, Q.-Q. Ni, N. Ohsako, and M. Iwamoto, *Composites A*, **35**, 1065 (2004).
15. W. Wang, P. Ping, X. Chen, and X. Jing, *Eur. Polym. J.*, **42**, 1240 (2006).
16. H. Tobushi, R. Matsui, S. Hayashi, and D. Shimada, *Smart Mater. Struct.*, **13**, 881 (2004).
17. F. Li, X. Zhang, J. Hou, M. Xu, X. Luo, D. Ma, and B.K. Kim, *J. Appl. Polym. Sci.*, **64**, 1511 (1997).
18. H.M. Jeong, B.K. Kim, and Y.J. Choi, *Polymer*, **41**, 1849 (2000).
19. K. Gall, P. Kreiner, D. Turner, and M. Hulse, *J. Microelectromech. Syst.*, **13**, 472 (2004).
20. Y. Liu, K. Gall, M.L. Dunn, A.R. Greenberg, and J. Diani, *Int. J. Plast.*, **22**, 279 (2006).
21. Y. Liu, K. Gall, M.L. Dunn, and P. McCluskey, *Mech. Mater.*, **36**, 929 (2004).
22. K. Gall, M.L. Dunn, Y. Liu, G. Stefanic, and D. Balzar, *Appl. Phys. Lett.*, **85**, 290 (2004).
23. V.A. Beloshenko, Y.E. Beigelzimer, A.P. Borzenko, and V.N. Varyukhin, *Mech. Comp. Mater.*, **39**, 255 (2003).
24. J. Diani, Y. Liu, and K. Gall, *Polym. Eng. Sci.*, **46**, 486 (2006).
25. V.A. Beloshenko, V.N. Varyukhin, and Y.V. Voznyak, *Composites A*, **36**, 65 (2005).
26. H.A. Khonakdar, S.H. Jafari, S. Rasouli, J. Morshedian, and H. Abedini, *Macromol. Theory Simul.*, **16**, 43 (2007).
27. C. Liu, S.B. Chun, P.T. Mather, L. Zheng, E.H. Haley, and E.B. Coughlin, *Macromolecules*, **35**, 9868 (2002).
28. H.M. Jeong, S.H. Lee, K.J. Cho, Y.T. Jeong, K.K. Kang, and J.K. Oh, *J. Appl. Polym. Sci.*, **84**, 1709 (2002).
29. V. Skákalová, V. Lukeš, and M. Breza, *Macromol. Chem. Phys.*, **198**, 3161 (1997).
30. F. Li, Y. Chen, X. Zhang, and M. Xu, *Polymer*, **39**, 6929 (1998).
31. M. Wang and L. Zhang, *J. Appl. Polym. Sci. Part B: Polym. Phys.*, **37**, 101 (1999).
32. B.C. Chun, S.H. Cha, C. Park, Y.-C. Chung, M.J. Park, and J.W. Cho, *J. Appl. Polym. Sci.*, **90**, 3141 (2003).
33. C. Park, J.Y. Lee, B.C. Chun, Y.-C. Chung, J.W. Cho, and B.G. Cho, *J. Appl. Polym. Sci.*, **94**, 308 (2004).
34. S.V. Ahir and E.M. Terentjev, *Nat. Mater.*, **4**, 491 (2005).
35. R. Vaia, *Nat. Mater.*, **4**, 429 (2005).
36. Z.G. Wei, R. Sandström, and S. Miyazaki, *J. Mater. Sci.*, **33**, 3743 (1998).
37. B. Winzek, S. Schmitz, H. Rumpf, T. Sterzl, R. Hassdorf, S. Thienbaus, J. Feydt, M. Moske, and E. Quandt, *Mater. Sci. Eng. A*, **378**, 40 (2004).
38. F. Li, L. Qi, J. Yang, M. Xu, X. Luo, and D. Ma, *J. Appl. Polym. Sci.*, **75**, 68 (2000).
39. C.-S. Zhang and Q.-Q. Ni, *Compos. Struct.*, **78**, 153 (2007).
40. C. Liu and P.T. Mather, *Mater. Res. Soc. Symp. Proc.*, **855E**, W4.7.1 (2005).
41. M.Y. Razzaq and L. Frormann, *Polym. Compos.*, **28**, 287 (2007).
42. J.R. Lin and L.W. Chen, *J. Appl. Polym. Sci.*, **69**, 1563 (1998).
43. T. Mirfakhrai, J.D.W. Madden, and R.H. Baughman, *Mater. Today*, **10**, 30 (2007).
44. Y. Wang, Y. Hu, X. Gong, W. Jiang, P. Zhang, and Z. Chen, *J. Appl. Polym. Sci.*, **103**, 3143 (2007).
45. T.J. Luand and A.G. Evans, *Sens. Actuators A*, **99**, 290 (2002).
46. A. Lendlein, H. Jiang, O. Jünger, and R. Langer, *Nature*, **434**, 879 (2005).

 DOI 10.1002/pen

47. K.D. Harris, C.W.M. Bastiaansen, and D.J. Broer, *J. Microelectromech. Syst.*, **16**, 480 (2007).
48. C. Liu, H. Qin, and P.T. Mather, *J. Mater. Chem.*, **17**, 1543 (2007).
49. K. Sakurai, Y. Shirakawa, T. Kashiwagi, and T. Takahashi, *Polymer*, **35**, 4238 (1994).
50. F. Li, W. Zhu, X. Zhang, C. Zhao, and M. Xu, *J. Appl. Polym. Sci.*, **71**, 1063 (1999).
51. Z. Hu, Y. Chen, C. Wang, Y. Zheng, and Y. Li, *Nature*, **393**, 149 (1998).
52. Y. Osada and A. Matsuda, *Nature*, **376**, 219 (1995).
53. R.V. Ulijn, N. Bibi, V. Jayawarna, P.D. Thornton, S.J. Todd, R.J. Mart, A.M. Smith, and J.E. Gough, *Mater. Today*, **10**, 40 (2007).
54. F.H. Gojny, M.H.G. Wichmann, B. Fiedler, I.A. Kinloch, W. Bauhofer, A.H. Windle, and K. Schulte, *Polymer*, **47**, 2036 (2006).
55. B. Weidenfeller, M. Hofer, and F.R. Schilling, *Composites A*, **35**, 423 (2004).
56. G.-W. Lee, M. Park, J. Kim, J. Lee, and H.G. Yoon, *Composites A*, **37**, 727 (2006).
57. Y.-M. Chen and J.-M. Ting, *Carbon*, **40**, 359 (2002).
58. M. Moniruzzaman and K.I. Winey, *Macromolecules*, **39**, 5194 (2006).
59. J.-H. Du, J. Bai, and H.-M. Cheng, *Express Polym. Lett.*, **1**, 253 (2007).
60. J.N. Coleman, U. Khan, and Y.K. Gun'ko, *Adv. Mater.*, **18**, 689 (2006).
61. I. Vir Singh, M. Tanaka, and M. Endo, *Int. J. Therm. Sci.*, **46**, 842 (2007).
62. J. Hone, M.C. Llaguno, M.J. Biercuk, A.T. Johnson, B. Batlogg, Z. Benes, and J.E. Fisher, *Appl. Phys. A: Mater. Sci. Proc.*, **74**, 339 (2002).
63. S.T. Huxtable, D.G. Cahill, S. Shenogin, L. Xue, R. Ozisik, P. Barone, M. Usrey, M.S. Strano, G. Siddons, M. Shim, and P. Keblinski, *Nat. Mater.*, **2**, 731 (2003).
64. S. Shenogin, A. Bodapati, L. Xue, R. Ozisik, and P. Keblinski, *Appl. Phys. Lett.*, **85**, 2229 (2004).
65. N. Shenogina, S. Shenogin, L. Xue, and P. Keblinski, *Appl. Phys. Lett.*, **87**, 1 (2005).
66. A. Yu, M.E. Itkis, E. Bekyarova, and R.C. Haddon, *Appl. Phys. Lett.*, **89**, 1 (2006).
67. F. Du, C. Guthy, T. Kashiwagi, J.E. Fisher, and K.I. Winey, *J. Polym. Sci. B: Polym. Phys.*, **44**, 1513 (2006).
68. F. Wu, X. He, Y. Zeng, and H.-M. Cheng, *Appl. Phys. A: Mater. Sci. Proc.*, **85**, 25 (2006).
69. J. Che, T. Çağin, and W.A. Goddard III, *Nanotechnology*, **11**, 65 (2000).
70. P.M. Ajayan and J.M. Tour, *Mater. Sci.*, **447**, 1066 (2007).
71. A. Bagchi and S. Nomura, *Compos. Sci. Technol.*, **66**, 1703 (2006).
72. T. Chen, G.J. Weng, and W.-C. Liu, *J. Appl. Phys.*, **97**, 1 (2005).
73. J. Morshedian, H.A. Khonakdar, and S. Rasouli, *Macromol. Theory Simul.*, **14**, 428 (2005).
74. A. Bhattacharyya and H. Tobushi, *Polym. Eng. Sci.*, **40**, 2498 (2000).